

Lattice fermion simulation of spontaneous time-reversal symmetry breaking in a helical Luttinger liquid

V. A. Zakharov, J. Sánchez Fernán, and C. W. J. Beenakker

Instituut-Lorentz, Universiteit Leiden, P.O. Box 9506, 2300 RA Leiden, The Netherlands

(Dated: January 2026)

We extend a recently developed “tangent fermion” method to discretize the Hamiltonian of a helical Luttinger liquid on a one-dimensional lattice, including two-particle backscattering processes that may open a gap in the spectrum. The fermion-doubling obstruction of the sine dispersion is avoided by working with a tangent dispersion, preserving the time-reversal symmetry of the Hamiltonian. The numerical results from a tensor network calculation on a finite lattice confirm the expectation from infinite-system analytics, that a gapped phase with spontaneously broken time-reversal symmetry emerges when the Fermi level is tuned to the Dirac point and the Luttinger parameter crosses a critical value.

I. INTRODUCTION

The edge of a quantum spin Hall insulator supports a time-reversally symmetric, one-dimensional metallic state in which spin and momentum are locked [1, 2]. This gapless phase realizes a helical Luttinger liquid [3–13], with time-reversal operation \mathcal{T} squaring to -1 , which is a distinct symmetry class from chiral or spinless Luttinger liquids [14]. A \mathbb{Z}_2 topological invariant forbids single-particle backscattering and prevents gap opening for the massless low-energy excitations [15]. The topological protection is lost if the edge is discretized with local couplings on a strictly one-dimensional (1D) lattice. In this sense the helical Luttinger liquid is “holographic” [3]: The 1D continuum theory emerges on the boundary of a 2D lattice.

Recent work [16–18] has shown that a 1D lattice formulation of the helical Luttinger liquid becomes possible for a *nonlocal* discretization of the momentum operator [19], resulting in a tangent dispersion $E \propto \tan(ka/2)$ instead of the usual sine dispersion $E \propto \sin ka$ (for lattice constant a and momentum $|k| < \pi/a$ in the first Brillouin zone). Such *tangent fermions* preserve time-reversal symmetry and spin-momentum locking, remaining in the symmetry class of a helical liquid without invoking a 2D bulk [20]. Most importantly, the nonlocality of the discretized Hamiltonian $H \propto \tan(ka/2)$ can be removed by working with a generalized eigenproblem [21], of the form $P\psi = EQ\psi$ with local operators $P \propto \sin ka$ and $Q \propto 1 + \cos ka$.

In the present work we extend the calculations of Ref. 17 to include more general two-particle interactions — both gap-preserving and gap-opening. It is known from bosonization analyses [3, 4], that strong interactions near half-filling (when the Fermi level is close to the Dirac point) can produce a pair of degenerate ground states, exchanged under \mathcal{T} , which gap the excitation spectrum. Here we recover that effect of spontaneous time-reversal symmetry breaking in a 1D lattice simulation, as an alternative to approaches that require a 2D lattice to realize the holographic liquid [22–26].

II. TANGENT FERMION LUTTINGER LIQUID

A. Continuum formulation

We summarize the continuum Hamiltonian of a helical Luttinger liquid [3–6].

We consider the edge of a quantum spin Hall insulator, along the x -axis, with fermionic field operators $\psi_\uparrow(x), \psi_\downarrow(x)$. Spin-up and spin-down electrons are counter-propagating (helical motion, with spin-momentum locking). We assume that spin-up electrons move to the right and spin-down electrons move to the left. The free Hamiltonian in the continuum is

$$H_0 = v_F \int dx (\psi_\uparrow^\dagger p \psi_\uparrow - \psi_\downarrow^\dagger p \psi_\downarrow), \quad (2.1)$$

with v_F the Fermi velocity and $p = -i\hbar\partial/\partial x \equiv -i\hbar\partial_x$ the momentum operator.

The time-reversal operation \mathcal{T} , squaring to -1 , transforms the field operators as

$$\psi_\uparrow(x) \mapsto \psi_\downarrow(x), \quad \psi_\downarrow(x) \mapsto -\psi_\uparrow(x). \quad (2.2)$$

Because also $p \mapsto -p$, the time-reversal operation leaves H_0 invariant. A single-particle spin-flip term, of the form

$$H_{\text{flip}} = g_{\text{flip}} \int dx [\psi_\uparrow^\dagger(x)\psi_\downarrow(x) + \psi_\downarrow^\dagger(x)\psi_\uparrow(x)], \quad (2.3)$$

changes sign under \mathcal{T} — so it is forbidden if time-reversal symmetry is preserved (zero magnetic field, no magnetic impurities). Since the spin-flip changes the direction of motion, time-reversal symmetry prevents single-particle backscattering in the helical edge state.

Electron-electron interactions enable forward scattering processes, either within a single spin band (intra-band) or between the spin bands (inter-band). The corresponding interaction Hamiltonians are

$$H_{\text{inter}} = g_{\text{inter}} \int dx \rho_\uparrow(x)\rho_\downarrow(x), \quad (2.4)$$

$$H_{\text{intra}} = g_{\text{intra}} \int dx [\rho_\uparrow(x)\rho_\uparrow(x) + \rho_\downarrow(x)\rho_\downarrow(x)], \quad (2.5)$$

with $\rho_\sigma(x) = \psi_\sigma^\dagger(x)\psi_\sigma(x)$: the normally ordered spin- σ number density.¹

Interactions also enable backscattering without breaking time-reversal symmetry, via two types of ‘‘Umklapp’’ processes, in which one particle (U1) or two particles (U2) change direction of motion:

$$H_{U2} = g_{U2} \int dx [\psi_\uparrow^\dagger(x)\psi_\downarrow(x)\psi_\uparrow^\dagger(x)\psi_\downarrow(x) + \psi_\downarrow^\dagger(x)\psi_\uparrow(x)\psi_\downarrow^\dagger(x)\psi_\uparrow(x)], \quad (2.6)$$

$$H_{U1} = ig_{U1} \int dx [\rho_\uparrow(x) - \rho_\downarrow(x)] \times [\psi_\downarrow^\dagger(x)\psi_\uparrow(x) - \psi_\uparrow^\dagger(x)\psi_\downarrow(x)]. \quad (2.7)$$

B. Lattice formulation

On a 1D lattice we discretize the momentum operator $p = -i\hbar\partial/\partial x$ by means of Stacey’s long-range finite difference [19],

$$p\psi(x) \mapsto -\frac{2i\hbar}{a} \sum_{n=1}^{\infty} (-1)^n [\psi(x-na) - \psi(x+na)]. \quad (2.8)$$

The non-locality can be removed by noting that Eq. (2.8) can be written equivalently as [21]

$$p\psi \mapsto \frac{2\hbar}{a} \frac{\sin \hat{k}a}{1 + \cos \hat{k}a} \psi, \quad e^{i\hat{k}a} f(x) = f(x+a). \quad (2.9)$$

The nonlocal Schrödinger equation $H_0\psi = E\psi$ therefore transforms into a *local* generalized eigenproblem upon substitution of $\psi = (1 + \cos \hat{k}a)\psi'$.

These lattice fermions (‘‘tangent fermions’’) have a tangent dispersion relation

$$E(k) = (2\hbar v_F/a) \tan(ka/2), \quad (2.10)$$

with a single Dirac point in the Brillouin zone $|k| < \pi/a$ (no fermion doubling). On a lattice of L sites, we impose periodic boundary conditions with odd L , or anti-periodic boundary conditions with even L , so that the discrete wave numbers avoid the pole at $|k| = \pi/a$.

The free Hamiltonian (2.1) with discretization (2.8) becomes

$$H_0 = \sum_{n>m} t_{nm} (c_{n\uparrow}^\dagger c_{m\uparrow} - c_{n\downarrow}^\dagger c_{m\downarrow}) + \text{H.c.}, \quad (2.11)$$

$$t_{nm} = 2it_0(-1)^{n-m}, \quad t_0 = \hbar v_F/a,$$

in terms of the fermion creation and annihilation operators $c_{n\sigma}, c_{n,\sigma}^\dagger$. The inter-band and intra-band interactions are

$$H_{\text{inter}} = t_{\text{inter}} \sum_n \rho_{n\uparrow} \rho_{n\downarrow}, \quad \rho_{n\sigma} = c_{n\sigma}^\dagger c_{n\sigma}, \quad (2.12)$$

$$H_{\text{intra}} = t_{\text{intra}} \sum_n (\rho_{n\uparrow} \rho_{n+1,\uparrow} + \rho_{n\downarrow} \rho_{n+1,\downarrow}), \quad (2.13)$$

$$t_{\text{inter}} = g_{\text{inter}}/a, \quad t_{\text{intra}} = \frac{1}{2} g_{\text{intra}}/a. \quad (2.14)$$

The factor of two in the relation between t_{intra} and g_{intra} appears when the point-splitting operation is regularized on the lattice (see App. A).

Similarly, the lattice regularization of the backscattering processes (2.6) and (2.7) is

$$H_{U2} = t_{U2} \sum_n [c_{n\uparrow}^\dagger c_{n\downarrow} c_{n+1,\uparrow}^\dagger c_{n+1,\downarrow} + c_{n\downarrow}^\dagger c_{n\uparrow} c_{n+1,\downarrow}^\dagger c_{n+1,\uparrow}], \quad (2.15)$$

$$H_{U1} = it_{U1} \sum_n [(\rho_{n+1,\uparrow} - \rho_{n+1,\downarrow})(c_{n\uparrow}^\dagger c_{n\downarrow} - c_{n\downarrow}^\dagger c_{n\uparrow}) + (\rho_{n\downarrow} - \rho_{n\uparrow})(c_{n+1,\uparrow}^\dagger c_{n+1,\downarrow} - c_{n+1,\downarrow}^\dagger c_{n+1,\uparrow})], \quad (2.16)$$

$$t_{U2} = \frac{1}{2} g_{U2}/a, \quad t_{U1} = \frac{1}{2} g_{U1}/a. \quad (2.17)$$

To check the time-reversal invariance, note that \mathcal{T} transforms $\rho_{n\uparrow} \mapsto \rho_{n\downarrow}$ and $ic_{n\downarrow}^\dagger c_{n\uparrow} \mapsto ic_{n\uparrow}^\dagger c_{n\downarrow}$.

C. Matrix product operator representation

The lattice formulation makes it possible to treat the interactions numerically on a tensor network [27–29], in which the Hamiltonian is represented by a matrix product operator (MPO): A product of matrices $M^{(n)}$ of fermion operators acting only on site n . Such an approach is efficient if the rank of each matrix (the bond dimension) is fixed — not growing with the number of sites L .

An exact MPO representation at fixed bond dimension is possible even if the Hamiltonian is nonlocal, provided that the generalized eigenproblem is local [17, 18]. Thus the tangent fermion Hamiltonian (2.11) has MPO representation [17]

$$H_0 = 2it_0 [M^{(1)} M^{(2)} \dots M^{(L)}]_{1,6}, \quad (2.18a)$$

$$M^{(n)} = \begin{pmatrix} 1 & c_{n\uparrow} & c_{n\uparrow}^\dagger & c_{n\downarrow} & c_{n\downarrow}^\dagger & 0 \\ 0 & -1 & 0 & 0 & 0 & c_{n\uparrow}^\dagger \\ 0 & 0 & -1 & 0 & 0 & c_{n\uparrow} \\ 0 & 0 & 0 & -1 & 0 & -c_{n\downarrow}^\dagger \\ 0 & 0 & 0 & 0 & -1 & -c_{n\downarrow} \\ 0 & 0 & 0 & 0 & 0 & 1 \end{pmatrix}, \quad (2.18b)$$

of L -independent bond dimension 6.

The tensor network calculation then proceeds as described in Ref. 17. Fermionic statistics is implemented by means of the Jordan-Wigner transformation. The ground

¹ The product of field operators at the same position is regularized by a point-splitting operation. We will instead use a lattice regularization, where the operators are evaluated at neighbouring sites, see App. A.

state wave function Ψ is represented by a matrix product state (MPS) and the DMRG algorithm (density matrix renormalization group [29]) from the TeNPy Library [30] is used to variationally minimize $\langle \Psi | H | \Psi \rangle / \langle \Psi | \Psi \rangle$. The bond dimension χ of the MPS is increased until convergence is reached. Our computer codes are available in a repository [31].

The Luttinger liquid is simulated at zero temperature and at fixed particle number $N = N_\uparrow + N_\downarrow$ (canonical ensemble). The half-filled band (zero chemical potential, Fermi level aligned with Dirac point) corresponds to $N = L$. Anti-periodic boundary conditions are implemented with L even, so that $N_\uparrow = N_\downarrow = L/2$ are equal at half-filling.²

Spurious oscillations of the wave function on even and odd lattice sites are removed by averaging the fermionic operators $c_{n\sigma}$ over nearby lattice sites,

$$\bar{c}_{n\sigma} = \frac{1}{2}c_{n\sigma} + \frac{1}{2}c_{n+1,\sigma}. \quad (2.19)$$

Smoothed correlators are then obtained from the ground state expectation values

$$\begin{aligned} \bar{C}_\sigma(n, m) &= \langle \bar{c}_{n\sigma}^\dagger \bar{c}_{m\sigma} \rangle, \\ \bar{R}_\alpha(n, m) &= \frac{1}{4} \langle \bar{c}_n^\dagger \sigma_\alpha \bar{c}_n \bar{c}_m^\dagger \sigma_\alpha \bar{c}_m \rangle, \end{aligned} \quad (2.20)$$

defined in terms of the spinor $\mathbf{c} = (c_\uparrow, c_\downarrow)$ and Pauli matrices σ_α .

III. RESULTS FOR FORWARD SCATTERING

If we only include forward scattering ($t_{U1} = 0 = t_{U2}$), the bosonization theory of an infinite Luttinger liquid [14, 32] gives a power law decay of the zero-temperature, zero-chemical-potential correlators,³

$$\begin{aligned} C_\sigma(x, x') &\propto |x - x'|^{-(1/2)(K+1/K)}, \\ R_x(x, x'), R_y(x, x') &\propto |x - x'|^{-2K}, \\ R_z(x, x') &\propto |x - x'|^{-2}, \end{aligned} \quad (3.1)$$

with Luttinger parameter K given by

$$\begin{aligned} K &= \sqrt{\frac{1 + \kappa_{\text{intra}} - \kappa_{\text{inter}}}{1 + \kappa_{\text{intra}} + \kappa_{\text{inter}}}}, \\ \kappa_{\text{inter}} &= \frac{t_{\text{inter}}}{2\pi t_0}, \quad \kappa_{\text{intra}} = \frac{2t_{\text{intra}}}{\pi t_0}. \end{aligned} \quad (3.2)$$

The Fermi velocity is renormalized according to

$$v = v_F \sqrt{(1 + \kappa_{\text{intra}})^2 - \kappa_{\text{inter}}^2}. \quad (3.3)$$

² In Ref. 17 we took periodic boundary conditions with L odd. In that case a half-filled band corresponds to different $N_\uparrow = (L+1)/2$ and $N_\downarrow = (L-1)/2$.

³ Notice the factor of four difference in the definitions of κ_{inter} and κ_{intra} : one factor of two comes from the sum over both spin directions in Eq. (2.13), the other factor of two comes from Eq. (2.14).

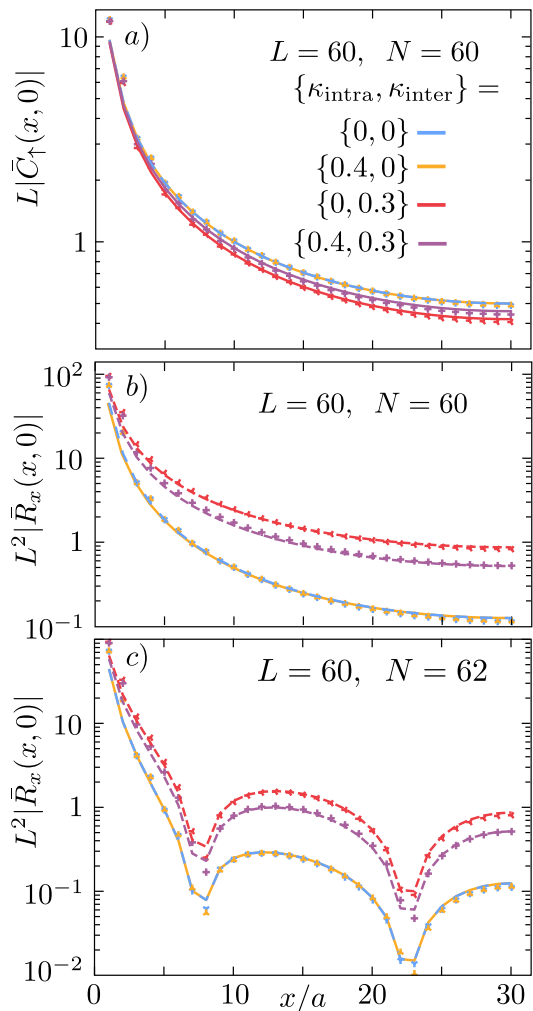


FIG. 1. Absolute value of the propagator \bar{C}_\uparrow and transverse spin correlator \bar{R}_x , defined in Eq. (2.20), calculated in the tensor network of $L = 60$ sites (MPS bond dimension $\chi = 8192$). The data points are computed from the tangent discretization of the Luttinger Hamiltonian, for free fermions and for a repulsive intra-band and inter-band interaction. Only forward scattering is included in this figure ($t_{U1} = 0 = t_{U2}$). The curves are the analytical results in the continuum from bosonization theory. Panels a) and b) are for a half-filled band ($N = L$). Panel c) shows \bar{R}_x away from half filling ($N = L + 2$). The corresponding data for \bar{C}_\uparrow is indistinguishable from panel a), so it is not included in the figure. For $\kappa_{\text{inter}} = 0$ the data is independent of κ_{intra} , hence blue and orange data overlaps.

We consider repulsive inter-band interactions, $t_{\text{inter}} > 0$, when $K \in (0, 1)$. The transverse spin correlators R_x and R_y then decay more slowly than the $1/x^2$ decay expected from a Fermi liquid. If there are only intra-band interactions ($t_{\text{inter}} = 0$) one has $K = 1$ and the correlators decay as for free electrons.

Numerical results are shown in Fig. 1 (data points). The curves are the continuum bosonization formulas (including finite-size corrections, see App. B). These results

generalize those presented in Ref. 17 by the inclusion of intra-band scattering. We show both the case of a half-filled band and results away from half-filling. The lattice numerics is in very good agreement with the continuum analytics, without any fit parameter.

IV. EFFECTS OF BACKSCATTERING

A. Gap opening

We next include backscattering, via nonzero t_{U1} or t_{U2} . The renormalization group analysis [3, 6] tells us that a gap will open in a half-filled band in the $L \rightarrow \infty$ limit, provided that $t_{U2} \neq 0$ and $K < K_c = 1/2$. The numerical results for a finite system shown in Figs. 2, 3, 4 are in agreement with this expectation.

In Fig. 2 we see that the propagator for a half-filled band follows the power law scaling law⁴

$$C_\sigma(x, 0) = L^{-(1/2)(K+1/K)} f_C(x/L) \quad (4.1)$$

of the gapless Luttinger liquid even in the presence of two-particle backscattering — provided that the Luttinger parameter $K \gtrsim 1/2$. A break down of the power law scaling occurs for smaller K , when the decay of the propagator approaches the exponential decay of a gapped liquid. The range of L that we can access numerically is not sufficiently large to precisely pinpoint the critical value of K , but the results are clearly consistent with $K_c = 1/2$.

Fig. 3 shows that a half-filled band is essential for the gap opening and Fig. 4 shows that single-particle backscattering does not open a gap — all consistent with the infinite-system analytics [3, 6].

B. Spontaneous time-reversal symmetry breaking

The gap opening by interactions is expected to be accompanied by spontaneous time-reversal symmetry breaking [3]: The emergence of a pair of degenerate ground states exchanged under \mathcal{T} , each of which introduces a nonzero mass term

$$M_\alpha(x) = \pm \frac{1}{2} \langle \psi^\dagger(x) \cdot \sigma_\alpha \cdot \psi(x) \rangle \quad (4.2)$$

in the effective Hamiltonian. This term changes sign upon \mathcal{T} , which is allowed by time-reversally symmetric interactions because it appears with opposite sign in the two ground states. Which mass term is produced by the two-particle interaction depends on its sign [3]: M_y if $t_{U2} > 0$ and M_x if $t_{U2} < 0$.

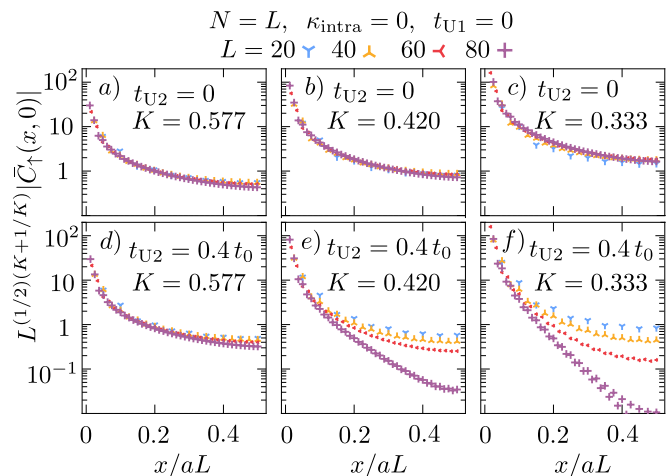


FIG. 2. Absolute value of the propagator \tilde{C}_\uparrow calculated in the tangent fermion tensor network for different L (MPS bond dimension $\chi = 2048$ for $L = 20$, $\chi = 4096$ for $L = 40, 60, 80$). For all panels, the band is half-filled ($N = L$). The top row includes only inter-band forward scattering, for three different values of $\kappa_{\text{inter}} = 0.5, 0.7, 0.8$, corresponding to the values of the Luttinger parameter K indicated in each panel. The lower row also includes two-particle backscattering ($t_{U2} = 0.4t_0$). The propagator is scaled by the power law (4.1), so that in a gapless liquid curves for different L collapse onto a single curve. This expected power law scaling breaks down in panels e) and f), with a crossover to an exponential decay indicating the opening of an excitation gap by two-particle backscattering for sufficiently strong forward scattering ($K < 0.5$).

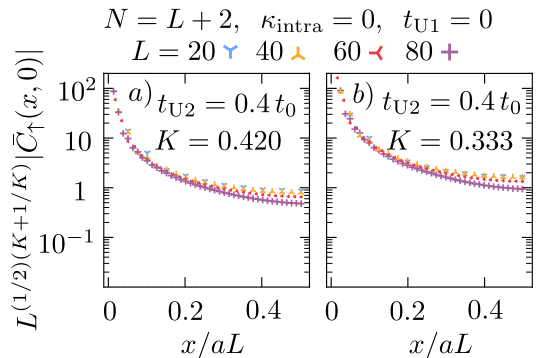


FIG. 3. Same as Figs. 2e) and 2f), but away from half-filling ($N = L + 2$). There is now no indication of a gap opening.

Since for large x the transverse spin correlator factorizes,

$$R_\alpha(x, x') \rightarrow M_\alpha(x)M_\alpha(x'), \quad |x - x'| \rightarrow \infty, \quad (4.3)$$

we can test for the appearance of a nonzero M_α by checking whether the correlator $R_\alpha(x, 0)$ saturates at a nonzero value for large x . Fig. 5 shows that this is indeed what happens, once K drops below $1/2$. Finally, Fig. 6 shows the emergence of a ground-state degeneracy in the gapped regime.

⁴ Since the decay of $C_\sigma(x, 0)$ with x for $L \rightarrow \infty$ should be independent of L , the scaling law (4.1) implies the power law decay (3.1) with x . The function f_C is given in App. B.

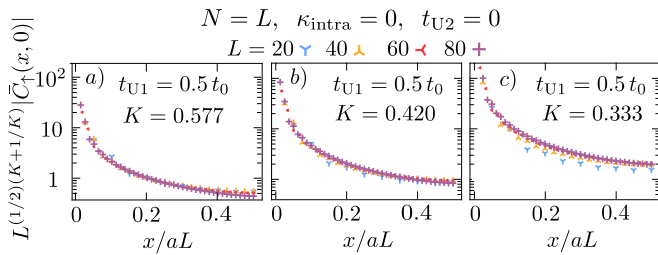


FIG. 4. Same as Figs. 2d), 2e), and 2f), but for $t_{U2} = 0$ and nonzero t_{U1} , to show that one-particle backscattering alone does not open a gap.

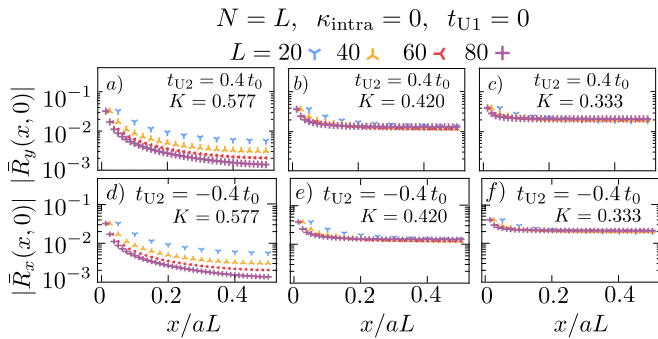


FIG. 5. Top row: Same as Figs. 2d), 2e), and 2f), but for the transverse spin correlator \bar{R}_y (no rescaling with L). The saturation of the correlator at a nonzero value in panels b), c) is a signature of spontaneous time-reversal symmetry breaking. The bottom row shows the same for negative t_{U2} , when the saturated correlator is \bar{R}_x instead of \bar{R}_y .

V. CONCLUSION

It was shown in Refs. 16–18 that a helical Luttinger liquid can be formulated and simulated directly on a one-dimensional lattice, without invoking the two-dimensional bulk that supports this “holographic” quantum liquid [3, 4]. By employing a tangent dispersion [19], supporting a *local* generalized eigenproblem [20, 21], fermion doubling is avoided while time-reversal symmetry and spin-momentum locking are retained at the lattice level.

Only the gapless phase of the Luttinger liquid was explored in these studies 16–18, a phase where closed-form analytical results from bosonization theory are available [14]. Here we show that the same framework makes it possible to study numerically the predicted [3–6] spontaneous time-reversal symmetry breaking and gap opening due to strong electron-electron interactions. Our results establish that the tangent-fermion regularization faithfully captures the low-energy physics of the helical Luttinger liquid, also in a regime where no closed-form analytical expressions are available.

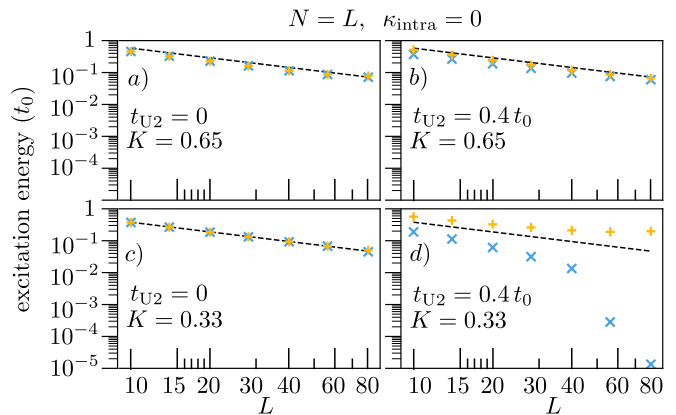


FIG. 6. Log-log plot of the energy above the ground state of the first two excited states, as a function of system size L . Panels a,b,c show an excitation energy ΔE that decays as expected for a gapless system: $\Delta E = 2\pi\hbar v/L$ (dashed line), with velocity v renormalized according to Eq. (3.3). Panel d) shows the signature of spontaneous time-reversal symmetry breaking due to a nonzero t_{U2} at $K < 1/2$: One of the two excited states (blue data points) becomes degenerate with the ground state, while the other excited state (yellow data points) levels off at a nonzero ΔE .

ACKNOWLEDGMENTS

We have benefited from discussions with A. S. Shankar. This work was supported by the Netherlands Organisation for Scientific Research (NWO/OCW), as part of Quantum Limits (project number SUMMIT.1.1016).

Appendix A: Lattice regularization of point splitting

1. Intra-band scattering

Point splitting [33, 34] is the operation that replaces the product of fermion fields at the same position by an infinitesimal displacement $\pm\epsilon$,

$$\psi_{\sigma}(x)\psi_{\sigma}(x) \mapsto \frac{1}{2}\psi_{\sigma}(x)\psi_{\sigma}(x+\epsilon) + \frac{1}{2}\psi_{\sigma}(x-\epsilon)\psi_{\sigma}(x). \quad (\text{A1})$$

To first order in ϵ , the right-hand-side inserts the derivative $\epsilon\psi(x)\partial_x\psi(x)$, which is how the point-splitting operation is usually introduced in the Luttinger Hamiltonian [5, 6].

The product of density operators appearing in H_{intra} is split into

$$\begin{aligned} \rho_{\sigma}(x)\rho_{\sigma}(x) &\mapsto \frac{1}{4}[\psi_{\sigma}^{\dagger}(x+\epsilon)\psi_{\sigma}^{\dagger}(x) + \psi_{\sigma}^{\dagger}(x)\psi_{\sigma}^{\dagger}(x-\epsilon)] \\ &\quad \times [\psi_{\sigma}(x)\psi_{\sigma}(x+\epsilon) + \psi_{\sigma}(x-\epsilon)\psi_{\sigma}(x)] \\ &= \frac{1}{4}\rho_{\sigma}(x)[\rho_{\sigma}(x+\epsilon) + \rho_{\sigma}(x-\epsilon)] \\ &\quad - \psi_{\sigma}^{\dagger}(x+\epsilon)\psi_{\sigma}(x-\epsilon) - \psi_{\sigma}^{\dagger}(x-\epsilon)\psi_{\sigma}(x+\epsilon). \end{aligned} \quad (\text{A2})$$

On the lattice we replace ϵ by the lattice spacing a . The integral over x in Eq. (2.5) is replaced by the sum

over sites of the operators $c_{n\sigma} = \sqrt{a}\psi_\sigma(x = na)$, resulting in

$$\begin{aligned} a \int dx \rho_\sigma(x)\rho_\sigma(x) &\mapsto \frac{1}{4} \sum_n \rho_{n\sigma} [\rho_{n+1,\sigma} + \rho_{n-1,\sigma} \\ &\quad - c_{n+1,\sigma}^\dagger c_{n-1,\sigma} - c_{n-1,\sigma}^\dagger c_{n+1,\sigma}] \\ &= \frac{1}{2} \sum_n \rho_{n\sigma} (\rho_{n+1,\sigma} - 1) + \frac{1}{4} \sum_n \rho_{n\sigma} J_{n\sigma}, \end{aligned} \quad (\text{A3})$$

where we have defined

$$J_{n\sigma} = 2\rho_{n\sigma} - c_{n+1,\sigma}^\dagger c_{n-1,\sigma} - c_{n-1,\sigma}^\dagger c_{n+1,\sigma}, \quad (\text{A4})$$

and we have used that $\rho_{n\sigma}^2 = \rho_{n\sigma}$.

The term $J_{n\sigma}$ is a discretized second derivative, in Fourier representation

$$\sum_n J_{n\sigma} = 2 \sum_k (1 - \cos 2ka) c_{k\sigma}^\dagger c_{k\sigma}, \quad (\text{A5})$$

so it vanishes $\propto (ka)^2$ in the long-wave length limit. To make contact with the bosonisation theory we ignore this term in the main text, representing the intra-band scattering by

$$\begin{aligned} H_{\text{intra}} &= \frac{1}{2} (g_{\text{intra}}/a) \sum_{n,\sigma} \rho_{n\sigma} (\rho_{n+1,\sigma} - 1) \\ &= t_{\text{intra}} \sum_{n,\sigma} \rho_{n\sigma} \rho_{n+1,\sigma} + t_{\text{intra}} N, \end{aligned} \quad (\text{A6})$$

with $t_{\text{intra}} = \frac{1}{2} g_{\text{intra}}/a$ and $N = \sum_{n,\sigma} \rho_{n\sigma}$. Since we work in the canonical ensemble, at fixed particle number N , the offset $t_{\text{intra}} N$ may be ignored, and we arrive at Eq. (2.13) from the main text.

2. Two-particle Umklapp scattering

In a similar manner, the product of operators $\chi(x) = \psi_\uparrow^\dagger(x)\psi_\downarrow(x)$ appearing in H_{U2} is split into

$$\begin{aligned} \chi(x)\chi(x) &\mapsto \frac{1}{4} [\psi_\uparrow^\dagger(x+\epsilon)\psi_\uparrow^\dagger(x) + \psi_\uparrow^\dagger(x)\psi_\uparrow^\dagger(x-\epsilon)] \\ &\quad \times [\psi_\downarrow(x)\psi_\downarrow(x+\epsilon) + \psi_\downarrow(x-\epsilon)\psi_\downarrow(x)] \\ &= \frac{1}{4} \chi(x) [\chi(x+\epsilon) + \chi(x-\epsilon) \\ &\quad - \psi_\uparrow^\dagger(x+\epsilon)\psi_\downarrow(x-\epsilon) - \psi_\uparrow^\dagger(x-\epsilon)\psi_\downarrow(x+\epsilon)], \end{aligned} \quad (\text{A7})$$

which on the lattice reduces to

$$\begin{aligned} a \int dx \chi(x)\chi(x) &\mapsto \frac{1}{4} \sum_n \chi_n [\chi_{n+1} + \chi_{n-1} \\ &\quad - c_{n+1,\uparrow}^\dagger c_{n-1,\downarrow} - c_{n-1,\uparrow}^\dagger c_{n+1,\downarrow}] \\ &= \frac{1}{2} \sum_n \chi_n \chi_{n+1} + \frac{1}{4} \sum_n \chi_n K_n, \end{aligned} \quad (\text{A8})$$

$$K_n = 2\chi_n - c_{n+1,\uparrow}^\dagger c_{n-1,\downarrow} - c_{n-1,\uparrow}^\dagger c_{n+1,\downarrow}, \quad (\text{A9})$$

with $\chi_n = c_{n\uparrow}^\dagger c_{n\downarrow}$ and $\chi_n^2 = 0$.

The term K_n is again a second derivative,

$$\sum_n K_n = 2 \sum_k (1 - \cos 2ka) c_{k\uparrow}^\dagger c_{k\downarrow}, \quad (\text{A10})$$

which becomes irrelevant in the long-wave length regime. We thus represent the two-particle Umklapp term (2.6) by the lattice regularization

$$H_{U2} = \frac{1}{2} (g_{U2}/a) \sum_n [c_{n\uparrow}^\dagger c_{n\downarrow} c_{n+1,\uparrow}^\dagger c_{n+1,\downarrow} + \text{H.c.}], \quad (\text{A11})$$

which is Eq. (2.15) in the main text.

3. Single-particle Umklapp scattering

For the H_{U1} interaction (2.7) the point splitting is of the form

$$\begin{aligned} \psi_\uparrow^\dagger(x)\psi_\uparrow^\dagger(x)\psi_\uparrow(x)\psi_\downarrow(x) &\mapsto \\ \frac{1}{2} [\psi_\uparrow^\dagger(x+\epsilon)\psi_\uparrow^\dagger(x) + \psi_\uparrow^\dagger(x)\psi_\uparrow^\dagger(x-\epsilon)] &\psi_\uparrow(x)\psi_\downarrow(x). \end{aligned} \quad (\text{A12})$$

The corresponding lattice regularization is

$$\begin{aligned} H &= \frac{1}{2} (g_{U1}/a) \sum_n [(\rho_{n+1,\uparrow} + \rho_{n\downarrow}) (i c_{n\uparrow}^\dagger c_{n+1,\downarrow} + \text{H.c.}) \\ &\quad - (\rho_{n+1,\downarrow} + \rho_{n\uparrow}) (i c_{n+1,\uparrow}^\dagger c_{n\downarrow} + \text{H.c.})]. \end{aligned} \quad (\text{A13})$$

To implement this as a matrix product operator it is more convenient if the spin-flip operators act on the same site. For that purpose we make the replacements $c_{n\sigma} \leftrightarrow c_{n+1,\sigma}$, with an error that vanishes as ka in the long-wave length limit. This gives

$$\begin{aligned} H_{U1} &= \frac{1}{2} (g_{U1}/a) \sum_n [(\rho_{n\downarrow} - \rho_{n\uparrow}) (i c_{n+1,\uparrow}^\dagger c_{n+1,\downarrow} + \text{H.c.}) \\ &\quad + (\rho_{n+1,\uparrow} - \rho_{n+1,\downarrow}) (i c_{n\uparrow}^\dagger c_{n\downarrow} + \text{H.c.})], \end{aligned} \quad (\text{A14})$$

which is Eq. (2.16) in the main text.

Appendix B: Bosonization results with finite-size corrections

If there is only forward scattering ($g_{U1} = 0 = g_{U2}$) the correlators in the continuum can be calculated analytically from bosonization theory [14, 32]. To compare with the numerics on a finite lattice we need to include finite-size corrections.

In the canonical ensemble at zero temperature the propagator C_σ and transverse spin correlators $R_x = R_y$ are given by [16, 17]

$$C_\sigma(x, 0) = \frac{\sigma e^{\delta N_\sigma (2\pi i x/L)}}{2\pi i a_* |(L/\pi a_*) \sin(\pi x/L)|^{(1/2)(K+1/K)}}, \quad (\text{B1a})$$

$$R_x(x, 0) = \frac{\cos(2\pi(\delta N_\uparrow + \delta N_\downarrow)x/L)}{2(2\pi a_*)^2 |(L/\pi a_*) \sin(\pi x/L)|^{2K}}, \quad (\text{B1b})$$

in a system of length L with antiperiodic boundary conditions and short-distance (UV) regularization constant a^* . The number δN_σ is the number of spin- σ electrons relative to a half-filled band. The Luttinger parameter K , dependent on the inter-band and intra-band forward

scattering strengths, is given by Eq. (3.2).

For the comparison with a lattice calculation the lengths x and L are measured in units of the lattice constant a . A comparison [17] of lattice and UV regularization gives $a = 2a^*$.

-
- [1] M. Z. Hasan and C. L. Kane, *Topological insulators*, Rev. Mod. Phys. **82**, 3045 (2010).
- [2] J. Maciejko, T. L. Hughes, and S.-C. Zhang, *The quantum spin Hall effect*, Annu. Rev. Condens. Matter Phys. **2**, 31 (2011).
- [3] C. Wu, B. A. Bernevig, and S.-C. Zhang, *Helical liquid and the edge of quantum spin Hall systems*, Phys. Rev. Lett. **96**, 106401 (2006).
- [4] C. Xu and J. E. Moore, *Stability of the quantum spin Hall effect: Effects of interactions, disorder, and \mathbb{Z}_2 topology*, Phys. Rev. B **73**, 045322 (2006).
- [5] N. Lezmy, Y. Oreg, and M. Berkooz, *Single and multiparticle scattering in helical liquid with an impurity*, Phys. Rev. B **85**, 235304 (2012).
- [6] N. Kainaris, I. V. Gornyi, S. T. Carr, and A. D. Mirlin, *Conductivity of a generic helical liquid*, Phys. Rev. B **90**, 075118 (2014).
- [7] M. Levin and A. Stern, *Fractional topological insulators*, Phys. Rev. Lett. **103**, 196803 (2009).
- [8] T. Neupert, L. Santos, S. Ryu, and C. Chamon, *Fractional topological liquids with time-reversal symmetry and their lattice realization*, Phys. Rev. B **84**, 165107 (2011).
- [9] Tingxin Li, Pengjie Wang, Hailong Fu, Lingjie Du, Kate A. Schreiber, Xiaoyang Mu, Xiaoxue Liu, Gerard Sullivan, Gábor A. Csáthy, Xi Lin, and Rui-Rui Du, *Observation of a helical Luttinger liquid in InAs/GaSb quantum spin Hall edges*, Phys. Rev. Lett. **115**, 136804 (2015).
- [10] G. Dolcetto, M. Sasseti, and T. L. Schmidt, *Edge physics in two-dimensional topological insulators*, Riv. Nuovo Cim. **39**, 113 (2016).
- [11] R. Stühler, F. Reis, T. Müller, T. Helbig, T. Schwemmer, R. Thomale, J. Schäfer, and R. Claesse, Nature Phys. **16**, 47 (2020).
- [12] C.-H. Hsu, P. Stano, J. Klinovaja, and D. Loss, *Helical liquids in semiconductors*, Semicond. Sci. Technol. **36**, 123003 (2021).
- [13] Junxiang Jia, Elizabeth Marcellina, Anirban Das, Michael S. Lodge, BaoKai Wang, Duc-Quan Ho, Riddhi Biswas, Tuan Anh Pham, Wei Tao, Cheng-Yi Huang, Hsin Lin, Arun Bansil, Shantanu Mukherjee, and Bent Weber, *Tuning the many-body interactions in a helical Luttinger liquid*, Nature Comm. **13**, 6046 (2022).
- [14] T. Giamarchi, *Quantum Physics in One Dimension* (Clarendon Press, Oxford, 2003).
- [15] C. L. Kane and E. J. Mele, \mathbb{Z}_2 Topological order and the quantum spin Hall effect, Phys. Rev. Lett. **95**, 146802 (2005).
- [16] V. A. Zakharov, J. Tworzydło, C. W. J. Beenakker, and M. J. Pacholski, *Helical Luttinger liquid on a space-time lattice*, Phys. Rev. Lett. **133**, 116501 (2024).
- [17] V. A. Zakharov, S. Polla, A. Donís Vela, P. Emonts, M. J. Pacholski, J. Tworzydło, and C. W. J. Beenakker, *Luttinger liquid tensor network: Sine versus tangent dispersion of massless Dirac fermions*, Physical Review Research **6**, 043059 (2024).
- [18] J. Haegeman, L. Lootens, Q. Mortier, A. Stottmeister, A. Ueda, and F. Verstraete, *Interacting chiral fermions on the lattice with matrix product operator norms*, arXiv:2405.10285
- [19] R. Stacey, *Eliminating lattice fermion doubling*, Phys. Rev. D **26**, 468 (1982).
- [20] C. W. J. Beenakker, A. Donís Vela, G. Lemut, M. J. Pacholski, and J. Tworzydło, *Tangent fermions: Dirac or Majorana fermions on a lattice without fermion doubling*, Annalen Physik **535**, 2300081 (2023).
- [21] M. J. Pacholski, G. Lemut, J. Tworzydło, and C. W. J. Beenakker, *Generalized eigenproblem without fermion doubling for Dirac fermions on a lattice*, SciPost Phys. **11**, 105 (2021).
- [22] M. Hohenadler, T. C. Lang, and F. F. Assaad, *Correlation effects in Quantum spin-Hall insulators: A quantum Monte Carlo study*, Phys. Rev. Lett. **106**, 100403 (2011); *Erratum*, Phys. Rev. Lett. **109**, 229902 (2012).
- [23] M. Hohenadler, Z. Y. Meng, T. C. Lang, S. Wessel, A. Muramatsu, and F. F. Assaad, *Quantum phase transitions in the Kane-Mele-Hubbard model*, Phys. Rev. B **85**, 115132 (2012).
- [24] Yixin Ma, Shenghan Jiang, and Chao Xu, *Variational tensor wavefunctions for the interacting quantum spin Hall phase*, Phys. Rev. Lett. **132**, 126504 (2024).
- [25] R. Soni, H. Radhakrishnan, B. Rosenow, G. Alvarez, and A. Del Maestro, *Topological and magnetic properties of the interacting Bernevig-Hughes-Zhang model*, Phys. Rev. B **109**, 245115 (2024).
- [26] R. Soni, M. Thamm, G. Alvarez, B. Rosenow, and A. Del Maestro, *Edge reconstruction in a quantum spin Hall insulator*, arXiv:2508.10726.
- [27] F. Verstraete, J. J. Garcia-Ripoll, and J. I. Cirac, *Matrix product density operators: Simulation of finite-temperature and dissipative systems*, Phys. Rev. Lett. **93**, 207204 (2004).
- [28] M. Zwolak and G. Vidal, *Mixed-state dynamics in one-dimensional quantum lattice systems: A time-dependent superoperator renormalization algorithm*, Phys. Rev. Lett. **93**, 207205 (2004).
- [29] U. Schollwöck, *The density-matrix renormalization group in the age of matrix product states*, Annals Physics **326**, 96 (2011).
- [30] J. Hauschild and F. Pollmann *Efficient numerical simulations with Tensor Networks: Tensor Network Python (TeNPy)*, SciPost Phys. Lect. Notes **5** (2018).
- [31] Computer codes are available at this Zenodo repository.
- [32] J. von Delft and H. Schoeller, *Bosonization for beginners — refermionization for experts*, Ann. Physik **510**, 225 (1998).
- [33] R. Shankar, *Quantum Field Theory and Condensed Matter* (Cambridge, 2017).
- [34] Juven Wang and Xiao-Gang Wen, *Solution to the 1 + 1*

dimensional gauged chiral Fermion problem, Phys. Rev. D **99**, 111501(R) (2019).